Bis- and *tris*(pyridyl)amine-oxidovanadium complexes: Characteristics and insulin-mimetic potential†

Jessica Nilsson,[a] Eva Degerman,[b] Matti Haukka,[c] George C. Lisensky,[d] Eugenio Garribba,[e] Yutaka Yoshikawa,[f] Hiromu Sakurai,[f] Eva A. Enyedy,[g] Tamás Kiss,[g] Hossein Esbak,[h] Dieter Rehder*[h] and Ebbe Nordlander*[a]

Received 20th February 2009, Accepted 22nd May 2009
First published as an Advance Article on the web 5th August 2009
DOI: 10.1039/b903456k

Two novel vanadium complexes, $[V^{IV}O(bp\text{-}O)(HSO_4)]$ (**1**) and $[V^{IV}O(bp\text{-}OH)Cl_2]\cdot CH_3OH$ (**2**·CH_3OH), where bp-OH is 2-{[bis(pyrid-2-yl)methyl]amine}methylphenol, were prepared and structurally characterised. EPR spectra of methanol solutions of **2** suggest exchange of Cl^- for CH_3OH and partial conversion to $[VO(bp\text{-}OH)(CH_3OH)_3]^{2+}$. Speciation studies on the VO^{2+}-bpOH system in a water/dmso mixture (4:1 v/v) revealed $[VO(bp\text{-}O)(H_2O)_n]^+$ as the dominating species in the pH range 2–7. The insulin-mimetic properties of **1** and **2**, $[V^{IV}O(SO_4)tpa]$ (**3**), $[V^{IV}O(pic\text{-}trpMe)_2]$ (**5**) and the new mixed-ligand complexes $[V^{V}O(pic\text{-}trpH)tpa]Cl_2$ (**4**Cl_2) and $[V^{V}O(pic\text{-}OEt)tpa]Cl_2$ (**6**Cl_2), tpa = tris(pyrid-2-yl)methylamine, picH-trpH = 2-carboxypyridine-5-(L-tryptophan)carboxamide (picH-trpMe is the respective tryptophanmethyl ester), pic-OEt = 5-carboethoxypyridine-2-carboxylic acid, were evaluated with rat adipocytes, employing two lipolysis assays (release of glycerol and free fatty acids (FFA)), respectively and a lipogenesis assay (incorporation of glucose into lipids). The IC_{50} values for the inhibition of lipolysis in the FFA assay vary between 0.41 (±0.03) (**5**) and 21.2 (±0.6) mM (**2**), as compared to 0.81 (±0.2) mM for $VOSO_4$.

Introduction

The average vanadium concentration in human blood plasma amounts to approximately 0.2 μM; tissue concentrations can go up to 6 μM.[1,2] The importance of the presence of vanadium in our body has been debated. It is considered a trace element, but so far no inherent biological function in humans has been reported. Based on its ability to inhibit many phosphatases,[3] it most likely functions as a regulator in phosphate metabolism. A functional role for vanadium has been established for marine macro-algae and some terrestrial fungi and lichen, which contain vanadium-dependent haloperoxidases, capable of catalysing the formation of hypohalous acid (or other {Hal^+} species) from halides, the oxygenation of thioethers to sulfoxides,[4] and other oxidation and oxygenations by peroxides.[1] Vanadium-nitrogenases present in bacteria and cyanobacteria are also known.[5]

At the end of the 19th century it was discovered that vanadium improves the state of patients suffering from diabetes mellitus.[6] *In vitro* studies confirming the effect of vanadium on glucose metabolism were published almost a century later.[7] Further studies revealed that sodium vanadate has a glucose lowering effect in blood plasma of rats suffering from chemically induced (by streptozotocin) diabetes.[8] Mechanisms of action are still insufficiently clear, but phosphate-like activity[3,7] and/or interference with phosphatases[9] has been suggested. However, the cellular targets for this activity are not fully understood; different phosphatases/kinases have been proposed.[7,9,10] Another question concerning the insulin-mimetic action of vanadium is that of the active species. Many of the vanadium compounds for which insulin-mimetic or insulin-enhancing effects have been validated, the families of maltolato[11] and picolinato complexes[12] in particular, have been shown to undergo ligand exchange in artificial sera, *i.e.* solutions, adjusted to physiological ionic strength, containing the main constituents of blood serum, *viz*. phosphate, citrate, lactate, oxalate, albumin and transferrin. Here, practically all of the vanadium is taken up by transferrin (Tf), the VO-Tf complex being incorporated by the cells *via* endocytosis. Under realistic physiological conditions, however, the transfer of the oxidovanadium(IV) or –(V) moiety from the genuine complex to transferrin can be kinetically hindered, increasing the life time to the extent where some of the complex carrying the original

[a]*Inorganic Chemistry Research Group, Chemical Physics, Center for Chemistry and Chemical Engineering, Lund University, SE-22100, Lund, Sweden. E-mail: Ebbe.Nordlander@chemphys.lu.se; Fax: +46 46 222 4119; Tel: +46 46 222 8118*
[b]*Department of Experimental Medical Science, Section for Diabetes, Metabolism and Endocrinology, Lund University, BMC C11, SE-221 84, Lund, Sweden*
[c]*Department of Chemistry, University of Joensuu, FI-80101, Joensuu, Finland*
[d]*Department of Chemistry, Beloit College, 700 College St., WI 53511, USA*
[e]*Department of Chemistry, University of Sassari, I-07100, Sassari, Italy*
[f]*Department of Analytical and Bioinorganic Chemistry, Kyoto Pharmaceutical University, Kyoto, 607-8414, Japan*
[g]*Department of Inorganic Chemistry, University of Szeged, H-6701, Szeged, Hungary*
[h]*Chemistry Department, University of Hamburg, D-20146 Hamburg, Germany. E-mail: rehder@chemie.uni-hamburg.de*

† Electronic supplementary information (ESI) available: Calculated (DFT) EPR parameters for **1** and **2**; assay results for **1**, **2** and **3** on glycerol release. CCDC reference numbers 688673 and 711845. For ESI and crystallographic data in CIF or other electronic format see DOI: 10.1039/b903456k

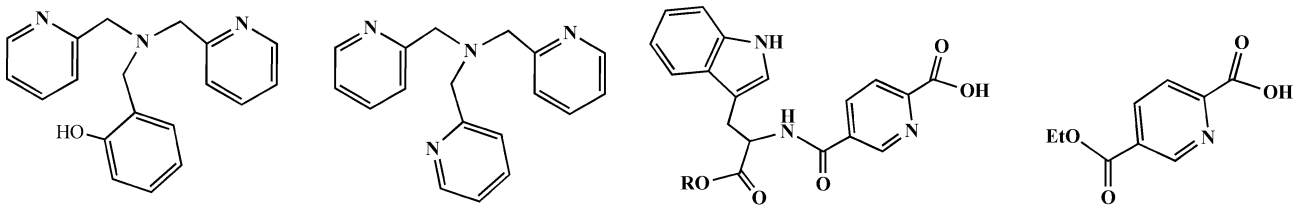

bp-OH **tpa** **picH-trpR (R = H, Me)** **picH-OEt**

Chart 1

ligand can enter the cell intact, again *via* endocytosis if the ligand is designed so as to be recognised by cell receptors, or *via* diffusion across the lipophilic membrane. The latter process has been demonstrated for pyrimidone complexes,[13] and can more generally be expected for stable complexes (with multidentate ligands) and an essentially hydrophobic ligand periphery. Once in the cytosol, the oxidovanadium moiety will be released, and since the cytosolic medium is reducing, vanadyl, VO^{2+}, is expected to dominate. The vanadyl form is supposed to be protected, at least in part, from intracellular re-oxidation by binding to cytosolic constituents, *e.g.* to glutathione.[14] On the other hand, vanadate(V), $H_2VO_4^-$, can be generated locally by reactive oxygen species. Vanadate, due to its phosphate-related properties, is believed to influence the function of proteins and activities of enzymes in insulin signalling pathways.[15]

In addition to the ambiguous mechanism of action, which impedes the straightforward design of potentially active complexes, there can also be problems with toxicity connected to the administration of vanadium as an (oral) anti-diabetic drug. The relatively poor absorption of vanadyl in the intestines (where VO^{2+} forms sparingly soluble hydroxides) can lead to stress in the gastrointestinal tract, ultimately causing symptoms such as diarrhoea or dehydration. To overcome this problem, organic ligands have been used. An organic ligand may—in addition to being advantageous for the transport across the intestinal mucosa, the transport within the blood stream, and across cell membranes—provide increased resistance to pH changes (which can be important for orally applied drugs) and possibly also influence cell recognition.[16,17] So far, only one vanadium complex, *bis*(ethylmaltolato)oxidovanadium(IV) (BEOV),[18] has completed phase 2 clinical trials in humans.[19]

Herein we report on new oxidovanadium(IV) complexes containing the tetradentate N,N,N,O-donor ligand *bis*(pyridylmethyl)-*o*-hydroxybenzylamine bp-OH (Chart 1) which, similarly to the related tripodal ligand *tris*(pyridylmethyl)amine (tpa),[20] forms stable complexes when coordinating to vanadium. Solution characteristics have been investigated by EPR and potentiometry. The crystal structures of two complexes, as well as *in vitro* studies with adipocytes, evaluating the insulin-mimetic effect of these new oxidovanadium complexes with respect to the inhibition of lipolysis and stimulation of lipogenesis, are presented. Complexes containing a mixed ligand sphere, *i.e.* 2,5-dipicolinates picH-trpR (trp = L-tryptophan), and picH-OEt, along with tpa (Chart 1), have been included in this study.

Results and discussion

Preparation and characterisation

The oxidovanadium complexes $[V^{IV}O(bp\text{-}O)HSO_4]$ (**1**), $[V^{IV}O(bp\text{-}OH)Cl_2]\cdot MeOH$ (**2**·MeOH), $[V^{V}O(pic\text{-}trpH)tpa]Cl_2$ (**4**Cl_2), and $[V^{V}O(pic\text{-}OEt)tpa]Cl_2$ (**6**Cl_2) were synthesised and characterised (*vide infra*). Their effect on lipogenesis (measured as incorporation of glucose derived metabolites into cellular lipids) and lipolysis (measured as the production of free fatty acids (FFA) and glycerol from triglycerides) was evaluated by testing on rat adipocytes along with the complex $[V^{IV}O(SO_4)tpa]$ (**3**)[17] and $[V^{IV}O(pic\text{-}trpMe)_2]$ (**5**).[12] Structural formulae of the six complexes are depicted in Fig. 1.

Complexes **1** and **2** were synthesised by stirring methanol solutions containing bp-OH and stoichiometric amounts of $VOSO_4\cdot 5H_2O$ or $VOCl_2$ (formed by the reaction of $VOSO_4$ with $BaCl_2$) at room temp. for about 12 h. The complexes exhibit an intense ν(V=O) IR resonance at 971 and 975 cm^{-1}, respectively, *i.e.* in the characteristic range[21] where appreciable intermolecular interactions involving the oxido ligand can be excluded. The results from mass spectrometry support the complex formation (m/z = 371 for **1** and 407 (see below) for **2**). For the preparation of **4**Cl_2, the ligand diester picMe-trpMe was deprotected by treatment with KOH in methanol to yield the potassium salt picK-trpK, which was converted to picH-trpH by addition of HCl. Addition of picH-trpH to a methanolic solution containing equimolar amounts of $VO(O\textit{i}Pr)_3$ and tpa·HCl yielded the cationic vanadium(V) complex, which was isolated in the form of its dichloride. Complex **4** shows a characteristic[22] $\delta(^{51}V)$ resonance at –485 ppm, and the ν(V=O) resonance at 978 cm^{-1}. $[VO(pic\text{-}OEt)tpa]Cl_2$ (**6**) was prepared accordingly from $VO(O\textit{i}Pr)_3$, 5-carboethoxypyridine-2-carboxylic acid (piH-OEt) and tpa; characteristic data: $\delta(^{51}V)$ = –489 ppm, ν(V=O) = 940 cm^{-1}.

The coordination environments of the complexes $[VO(bp\text{-}O)HSO_4]$ (**1**) and $[VO(bp\text{-}OH)Cl_2]$ (**2**) have also been revealed by X-ray crystal diffraction analysis. Selected bond lengths and angles are provided in Table 1 and ORTEP drawings of the complexes are shown in Fig. 2. The structure analysis reveals that in both complexes the ligand is coordinated *via* the two pyridyl nitrogens and the tertiary amine nitrogen, the latter in the axial position (*trans* to the oxido ligand). In **1** (Fig. 2, left), additional coordination by the phenolate oxygen occurs while in **2** (Fig. 2, right) the phenolic OH is dangling. The remaining coordination sites are occupied by HSO_4^- in **1**, and two Cl^- in **2**. While, in principle, coordination isomers of **1** are possible,[23a] there is no

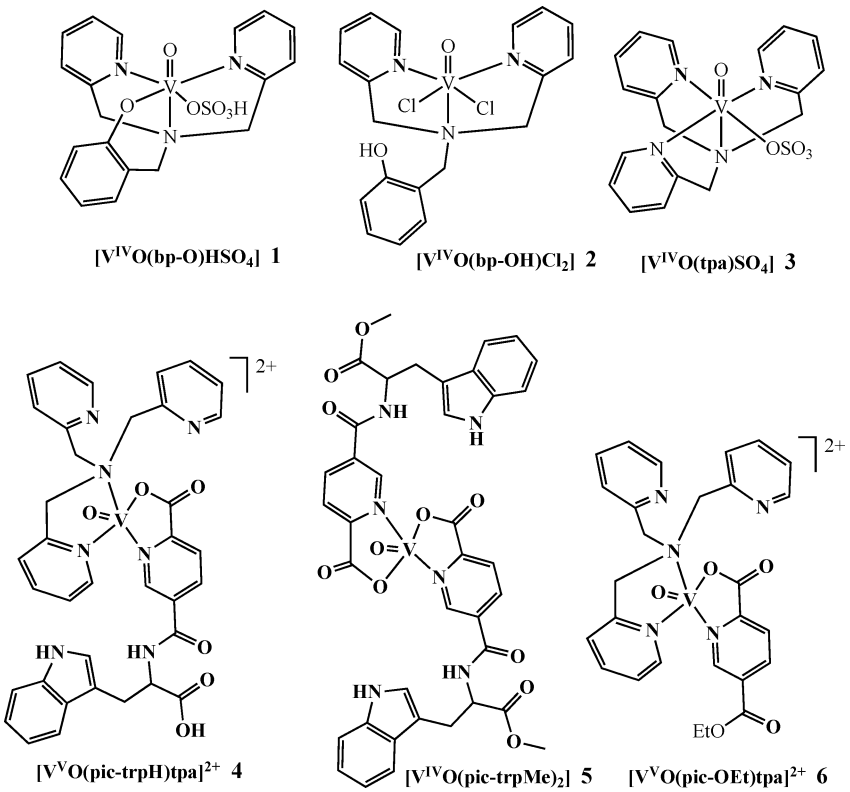

Fig. 1 Schematic representations of the complexes addressed in this work. For **3** and **5** see ref. 20 and 12, respectively; for the crystallographically determined structures of **1** and **2**·MeOH *cf*. Fig. 2.

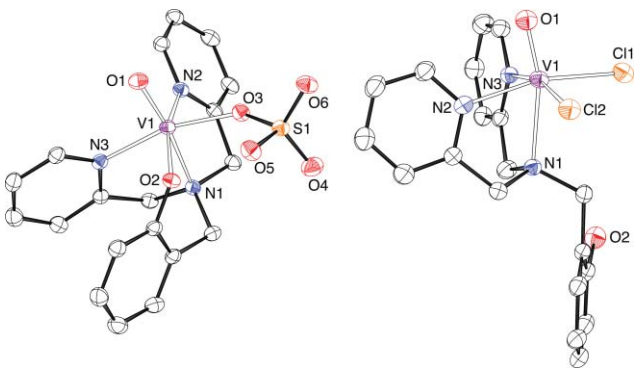

Fig. 2 ORTEP drawings of the complexes [VO(bp-O)HSO_4] (**1**, left) and the [VO(bp-OH)Cl_2] complex in **2**·MeOH (right).

Table 1 Selected bond lengths (Å) and angles (°) for [VO(bp-O)HSO_4] and [VO(bp-OH)Cl_2]·MeOH

	[VO(bp-O)HSO_4] (**1**)	[VO(bp-OH)Cl_2]·MeOH (**2**·MeOH)
V1–O1	1.6015(15)	1.6003(18)
V1–O2	1.9711(14)	—
V1–O3	2.0132(14)	—
V1–N1	2.3001(18)	2.380(2)
V1–N2	2.1166(17)	2.131(2)
V1–N3	2.1166(17)	2.114(2)
V1–Cl1	—	2.3540(7)
V1–Cl2	—	2.3400(8)
O2–C19	1.362(3)	—
O1–V1–N1	162.42(7)	163.63(9)
O2–V1–N3	87.21(6)	—
O3–V1–N2	84.25(6)	163.63(9)
O2–V1–O3	87.99(6)	—
N2–V1–N3	94.37(6)	84.93(8)
C19–O2–V1	122.43(12)	—
N2–V1–Cl2	—	89.35(6)
N3–V1–Cl1	—	89.19(6)
Cl1–V1–Cl2	—	92.37(3)

evidence of the existence of any other isomer than that which has been detected in the crystal structure, and in analogous MoO_2^+ [23a] and $FeCl_2^+$ complexes[23b] of bp-O$^-$. In **2**, bp-OH coordinates in a facial coordination mode, with the tertiary amine in the *trans* position to the oxido ligand, as expected. The complexes are, to a first approximation, octahedral. The axis O1–V–N1 is, however, somewhat bent (*cf*. the angle O1–V–N1 in Table 1), and vanadium is displaced from the mean plane spanned by the equatorial ligands by 0.338 (**1**) and 0.248 Å (**2**) towards the oxido ligand. The bond lengths are in good agreement with those reported for the related tpa complexes.[20] In **1**, the bond length $d(V–O_{phenolate}) = 1.9711(14)$ is shorter than $d(V–O_{hydrogensulfate}) = 2.0132(14)$ and the two $d(V–N_{pyridyl})$ (av. 2.153 Å). In both complexes, $d(V–N_{amine})$ is particularly long, 2.300(2) and 2.380(2) Å, respectively, as a consequence of the *trans* influence exerted by the oxido ligand. The OH (O5H) of the hydrogensulfato ligand in **1** is hydrogen bonded to the phenolate oxygen of the ligand; $d(O5H\cdots O2) = 2.531(2)$ Å. The methanol of crystallisation in **2**·MeOH is hydrogen-bonded to the two chlorido ligands; the respective bond lengths are $d(O3H\cdots Cl1) = 3.220(2)$ and $d(O3H\cdots Cl2) = 3.278(2)$ Å. An additional hydrogen bond, $d(O2H\cdots O3) = 2.685(3)$ Å, links the methanol to the phenol OH.

The EPR spectra of **1** and **2** exhibit patterns typical for vanadium(IV) species, *i.e.* an eight-line spectrum under isotropic,

Table 2 Experimental (refined by simulation) and calculated (based on DFT) anisotropic EPR parameters of complexes **1** (in water) and **2** (in methanol)[a]

	g_x and g_y	g_z	A_x and A_y	A_z	A_z calcd.[e]
1[b] $[VO(bp\text{-}O)HSO_4]/[VO(bp\text{-}O)H_2O]^+$	1.989	1.950	59.0	162.4	161.4/162.0
2[c] $[VO(bp\text{-}OH)Cl_2]/[VO(bp\text{-}OH)(CH_3OH)_2]^{2+}$	1.985	1.947	60.5	164.1	156.1/162.0
2[d] $[VO(bp\text{-}OH)(CH_3OH)Cl_2]/[VO(bp\text{-}OH)(CH_3OH)_3]^{2+}$	1.981	1.943	67.5	175.6	160.8/175.6

[a] A_x, A_y and A_z values in 10^{-4} cm^{-1}. For complex **2**, see Fig. 3. [b] [($N_{pyridyl}$, $N_{amine}{}^{ax}$, $N_{pyridyl}$, $O_{phenolate}$); $O_{hydrogensulfate}$ or H_2O] coordination. [c] Predominant species, likely with [($N_{pyridyl}$, $N_{amine}{}^{ax}$, $N_{pyridyl}$); CH_3OH; CH_3OH] coordination. [d] Minor species, [($N_{pyridyl}$, $N_{amine}{}^{ax}$); CH_3OH; CH_3OH; CH_3OH] coordination. [e] Calculated with the BHandHLYP functional and 6-311g(d,p) basis set.[27] For the complete data set of calcd. g and A values see ESI (Table S1†).

and two overlapping eight-line systems (for the parallel and perpendicular orientation) under anisotropic conditions; *cf*. Table 2. No splitting of the perpendicular component into an x and y subset was observed, excluding sizable rhombic or trigonal distortions. By comparing the experimental parallel hyperfine coupling constant A_z with that predicted on the basis of the "additivity rule" from the partial contribution of the equatorial ligand functions,[24] the coordination mode of the ligand bp-O^- found for $[V^{IV}O(bp\text{-}O)HSO_4]$ (**1**) by X-ray diffraction, *i.e.* ($N_{pyridyl}$, $N_{amine}{}^{ax}$, $N_{pyridyl}$, $O_{phenolate}$), was confirmed. EPR does not unambiguously allow for a distinction between hydrogensulfate and water as the fourth equatorial ligand, *i.e.* the species present in solution may also be $[VO(bp\text{-}O)H_2O]^+$. In view of the insulin-mimetic studies (see below), we have also measured the EPR spectrum of **1** in Hepes (4-(2-hydroxyethyl)-1-piperazineethanesulfonic acid) buffer, pH 7.4. The spectral parameters are the same as those obtained in methanol solution, indicating that in this aqueous medium the complex retains its integrity. Density functional theory (DFT) methods,[25] which have been demonstrated to be a powerful tool in the calculation of EPR parameters of $V^{IV}O$ species,[26,27] confirm this analysis.

The equatorial coordination mode for $[V^{IV}O(bp\text{-}OH)Cl_2]$ (**2**), on the other hand, was partially changed on dissolving the complex in methanol. The EPR spectrum shows two species (Fig. 3) in an approximate 9:1 ratio. The main species corresponds to that found for the solid state structure or, by exchange of the two chlorido ligands, to the related dication $[VO(bp\text{-}OH)(CH_3OH)_2]^{2+}$, while in the minor species, one of the equatorial $N_{pyridyl}$ is replaced by methanol,

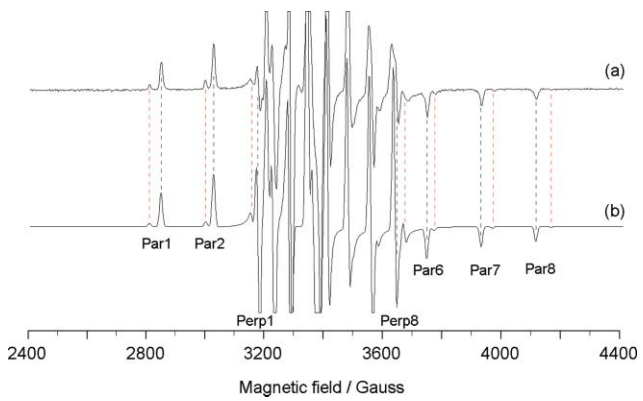

Fig. 3 Experimental (a) and simulated (b) anisotropic EPR spectrum of a methanol solution of $[VO(bp\text{-}OH)Cl_2]$ (**2**). The simulated spectrum was obtained by considering the percent amount of the main species (*cf*. Table 2 and text) to be 90%, that of the minor species 10%. With Par1, Par2, Par6, Par7 and Par8 the 1st, 2nd, 6th, 7th and 8th parallel transitions are indicated, with Perp1 and Perp8 the 1st and 8th perpendicular transitions.

resulting in the donor set [($N_{pyridyl}$, $N_{amine}{}^{ax}$); Cl; Cl; CH_3OH] (for a complex of composition $[VO(bp\text{-}OH)(CH_3OH)Cl_2]$), or [($N_{pyridyl}$, $N_{amine}{}^{ax}$); CH_3OH; CH_3OH; CH_3OH] in the case of complete exchange of chloride for methanol. An exchange of Cl^- for CH_3OH is also suggested by A_z values calculated on the basis of non-relativistic DFT methods (data in Tables 2 and S1†).[26,27] The coordination mode for the main species of **2** dissolved in methanol resembles that reported for a methanol solution of the complex $[VO(abpe)Cl_2]$ (abpe = amino-bis(2-pyridyl)methyl ethyl ether), for which a similar parallel coupling constant ($A_z = 165 \times 10^{-4}$ cm^{-1}) was reported.[28] In view of the speciation studies, which were carried out in buffer solution adjusted to an ionic strength of 0.2 M (KCl), we have also measured the EPR of compound **2** under the respective conditions. The parameters ($g_{x,y} = 1.985$, $g_z = 1.946$, $A_{x,y} = 163.8$, $A_z = 157.5 \cdot 10^{-4}$ cm^{-1}; no minor signal found) point to the presence of $[VO(bp\text{-}OH)Cl_2]$, which is not unexpected given the comparatively high concentration of chloride.

Complex **2** has also been studied by cyclic voltammetry, Fig. 4. The oxidation at 0.140 V *vs*. Fc/Fc^+ is quasi-reversible with $\Delta E_p =$ 110 mV for slower scan rates. The plot of peak current as a function of the square root of the scan rate (Fig. 4, inset) is linear for both the forward and reverse scans. This result indicates chemical reversibility, although it is not in itself sufficient evidence for such reversibility. An irreversible reduction at –0.65 V was also observed.

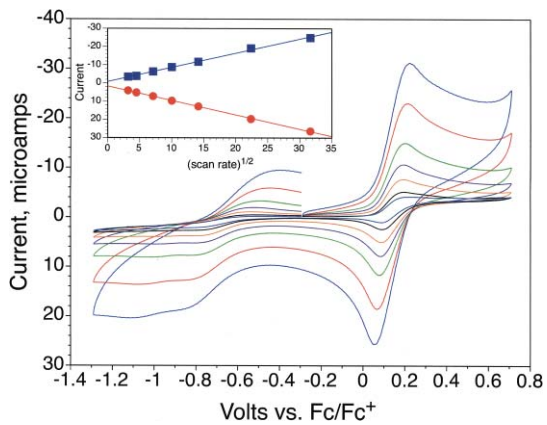

Fig. 4 CV of $[VO(bp\text{-}OH)Cl_2]$ (**2**) dissolved in CH_2Cl_2 (*ca*. 1 mM). Scan rates are 1000, 500, 200, 100, 50, 20 and 10 mV s^{-1}. The inset shows a plot of the peak current as a function of the square root of the scan rate for the forward and reverse scans.

Speciation studies

In the context of the lipolysis and lipogenesis assays with adipocytes described in the next section, the pH-dependent

Table 3 Protonation constants $\log\beta(H_iL)$ and pK_i values for L = bp-O$^-$,[a] and stability constants $\log\beta[(VO)_pL_qH_r]$ and pK values for its VO^{2+} complexes.[b]

$\log\beta$(HL) 10.93(2)	$\log\beta(H_2L)$ 16.58(3)	$\log\beta(H_3L)$ 20.12	
pK_1 3.54	pK_2 5.65	pK_3 10.93	
$\log\beta$(VOLH) 19.0(1)	$\log\beta$(VOL) 17.20(7)	$\log\beta(VOLH_{-1})$[c] 9.63(8)	$\log\beta(VOLH_{-2})$[c]
pK(VOLH) 1.8	pK(VOL) 7.57	p$K(VOLH_{-1})$ 10.4	0.8(1)

[a] Corresponding to the protonation/deprotonation of the two pyridine-N (i = 1 and 2) and the phenolic-O (i = 3). [b] Ionic strength 0.2 M(KCl), T = 25.0 °C, 20%(w/w) DMSO-H_2O. [c] The notation $VOLH_{-r}$ refers to the deprotonation of groups not titrable in the absence of the metal ion, or to water ligands in the coordination sphere of the complex $[VOL(H_2O)_n]$.

speciation of the ligands and complexes is of interest. Speciation studies were carried out by potentiometry in aqueous solution in the pH range 2–12 for the ligand bp-OH and the complexes it forms with VO^{2+}. Data are collated in Table 3 and Fig. 5.

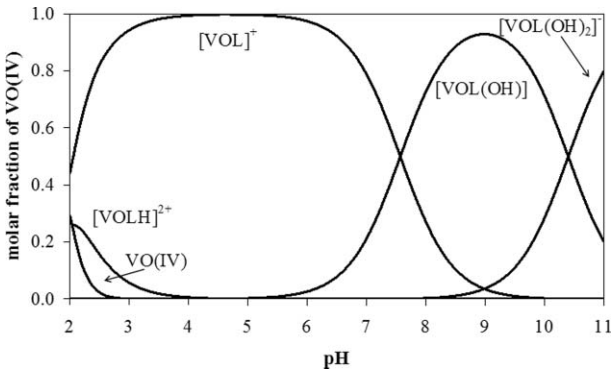

Fig. 5 Concentration distribution curves for the complexes formed in the VO^{2+}-L system, L = bp-OH, at a metal:ligand ratio of 1:2, $c(VO^{2+})$ = 1 mM. The species $[VOL(OH)_n]^{(n-1)-}$ corresponds to $VOLH_{-n}$ in Table 3.

Complex formation starts at a pH as low as 2, and the ligand also remains attached to VO^{2+} in the alkaline range, a stability which should be of some importance when it comes to potential oral applications of the complexes in the treatment of diabetes, where the compounds have to survive acidic conditions (pH of about 2 in the stomach) and slightly alkaline conditions (in the intestines and the blood stream). Overall, the vanadium-to-ligand stoichiometry remains 1:1; the dominating species in the acidic to neutral range is $[VOL]^+$.

Inhibition of lipolysis and stimulation of lipogenesis

For testing the insulin-mimetic properties of the complexes $[V^{IV}O(bp\text{-}O)HSO_4]$ (**1**), $[V^{IV}O(bp\text{-}OH)Cl_2]$ (**2**), $[V^{IV}O(tpa)SO_4]$ (**3**), $[V^{V}O(pic\text{-}trpH)tpa]^{2+}$ (**4**), $[V^{IV}O(pic\text{-}trpMe)_2]$ (**5**) and $[V^{V}O(pic\text{-}OEt)tpa]^{2+}$ (**6**), three assays were employed: two lipolysis assays, evaluating the breakdown of triglycerides, and a lipogenesis assay, evaluating the incorporation of glucose metabolites into cellular lipids. Insulin acts as both an inhibitor of lipolysis and a stimulator of lipogenesis.

Lipolysis leads to the release of glycerol and fatty acids from adipocytes as a result of triglyceride breakdown, mediated by hormones that increase *c*AMP (cyclic adenosine monophosphate) such as β adrenergic catecholamines.[29] The glycerol release was quantified by the method described by Moller and Roomi.[30] Upon stimulation of the adipocytes with isoprenaline, a β adrenergic receptor agonist, the release of glycerol is increased. This effect is counteracted by insulin. A similar but less pronounced effect is exerted by the simple salt $VOSO_4$ which, in Hepes buffer, is present as a VO^{2+}-aqua complex, apparently stabilised by Hepes. However, all three oxidovanadium coordination complexes (**1**, **2** and **3**) tested in this study lacked the ability to counteract isoprenaline-mediated glycerol release (for data see ESI, Fig. S1†). Alternatively, a lipolysis assay developed by Sakurai was employed,[31] in which the inhibition of lipolysis is followed by the amount of free fatty acids (FFA) released by rat adipocytes pre-treated with the catecholamine epinephrine (= adrenaline). These results are displayed in Fig. 6. The corresponding IC_{50} values, which define the concentration required for 50% inhibition of FFA release, are summarised in Table 4. Table 4 also contains IC_{50} values for ligands/pro-ligands. Except for picH-trpMe, the ligands themselves do not exhibit any effect. The ability of the pro-ligand picH-trp-Me to decrease the FFA release (and thus to

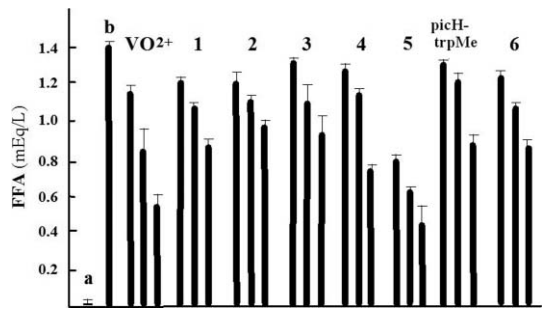

Fig. 6 Inhibitory effects of $VOSO_4$ (VO^{2+}), the pro-ligand picH-trpMe, and the vanadium complexes **1–6** on the free fatty acid (FFA) release from rat adipocytes treated with epinephrine. **a** = control group, *i.e.* cells treated with insulin; **b** = control group with epinephrine. The triplets of bars represent three different concentrations, *viz*. (from left to right) 0.1 mM, 0.5 mM and 1 mM. For **5**, see also ref. 12.

Table 4 IC_{50} values for the FFA release by vanadium complexes (*cf*. Fig. 6) and selected ligands/pro-ligands. $VOSO_4$ has been employed as the bench mark compound

Complexes	IC_{50} (mM) of complexes	Ligands/ligand precursors	IC_{50} (mM) of ligands[c]
$VOSO_4$	0.81 ± 0.2		
$[V^{IV}O(bp\text{-}O)HSO_4]$ **1**	3.85 ± 1.4	bp-OH	none
$[V^{IV}O(bp\text{-}OH)Cl_2]$ **2**	21.2 ± 6.9		
$[V^{IV}O(tpa)SO_4]$ **3**	4.60 ± 0.7	tpa	none
$[V^{V}O(pic\text{-}trpH)tpa]^{2+}$ **4**	1.84 ± 0.4	picH-trpMe	7.8 ± 3.9
$[V^{IV}O(pic\text{-}trpMe)_2]$ **5**	0.41 ± 0.03[a]; 0.33 ± 0.09[b]		
$[V^{V}O(pic\text{-}OEt)tpa]^{2+}$ **6**	15.1 ± 7.5	picH-OEt	none

[a] From ref. 12. [b] In the presence of ascorbic acid. [c] The entry "none" indicates that the effect compares to that of the control epinephrine, **b** in Fig. 6.

inhibit lipolysis) is, however, clearly less pronounced than for its vanadium complex [VO(pic-trpMe)$_2$] (**5**); and, although to a lesser extent, also in the mixed ligand complex **4**. For all of the complexes employed here some insulin-mimetic behaviour has been noted, in particular at concentrations of 1 mM. With the exception of **5**, the complexes are, however, less potent than the bench mark compound $VOSO_4$.

Glucose that is taken up by the adipocytes can be incorporated into lipids after it has been metabolized. Feeding cells tritium-labelled glucose (D-[6–^{3}H]-glucose) makes it possible to quantify this incorporation by scintillation. In the current study, both insulin and sodium vanadate (which, in aqueous solution at pH 7.4 and $c \approx 5$ mM, is mainly present as a mixture of ortho-, di- and tetravanadates) had a positive effect on the cellular glucose uptake, while the oxidovanadium complexes **1**, **2** and **3** as well as $VOSO_4$ did not show this effect. The results are shown in Fig. 7. Varying the concentration of the oxidovanadium complexes and $VOSO_4$, or prolonging the incubation time, did not affect the results. The inability of vanadyl sulfate to mediate glucose uptake by the cells in this assay is surprising in the light of previous findings that show that plasma glucose levels are lowered in diabetic rats that are administered $VOSO_4$ in drinking water,[1,32] suggesting that the vanadyl ion reaches the cytosol. One possible explanation for the lack of effect in this investigation is that extracellular interactions between glucose and VO^{2+} [33] prevent the transmembrane transport of VO^{2+}. The reasons that the oxidovanadium complexes **1**, **2** and **3**, with the bp-O(H) and tpa ligands, do not have an appreciable effect may have their origins in the stability of complexes with multidentate ligands, which prevents the release of vanadium species that can enter the cell. We have incubated adipocytes in Hepes buffer with $VOSO_4$ and with complex **1** and looked for EPR signals in the homogenates of the washed cells. Neither the hydrophilic fraction nor the fat cake (of the homogenate) contained detectable VO^{2+}, supporting the assumption that the lack of activity in this assay is due to the inability of the complexes to enter the cells.

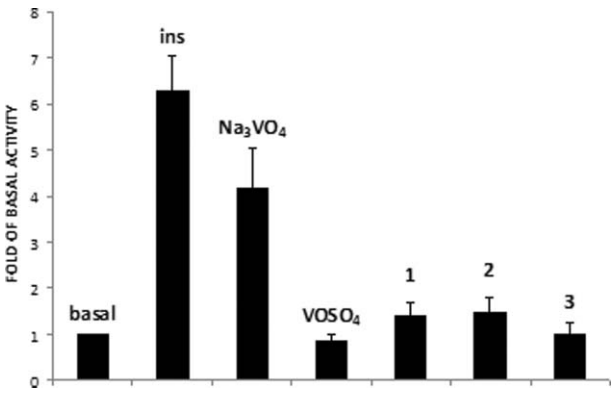

Fig. 7 The results of the lipogenesis assay are shown as the fold of basal activity, *i.e.* the activity with cells that have been treated solely with the labelled glucose (no additions were made to stimulate the glucose uptake). The following concentrations were used: insulin 1.7 nM, Na_3VO_4 5 mM, $VOSO_4$ 0.5 mM, complexes **1**, **2** and **3** 0.25 mM. Data are expressed as mean ± SEM, $n = 3$.

Conclusion

It has been shown earlier that in order to exert insulin-mimetic properties, oxidovanadium complexes should have at least one unoccupied coordination site or, alternatively, a site occupied by a monodentate, weakly coordinating ligand.[34] In this respect, complexes **1**, **2** and **3**, containing monodentate hydrogensulfate, chloride or sulfate, would have been expected to have insulin-mimetic properties. As we have noted in the Introduction, insulin-mimetic properties are also favoured by a balanced complex stability, balanced in the sense that the complex survives the passage through the gastro-intestinal tract (and, in part, transport with the blood serum), but also readily delivers the oxidovanadium moiety to another transporter, such as transferrin, recognisable to membrane receptors. In complexes **1**, **2** and **3**, the rigidity of the tri- to tetradentate ligand system appears to stabilise the complex to the extent where release of the ligand (or ligand exchange) does not take part to a sizable extent, or is kinetically disfavoured. The transmembrane transport *via* diffusion, as documented for pyrimidone complexes,[13] does not seem to take place or is too slow with our complexes. Consequently, complexes **1**, **2** and **3** did not exhibit an insulin-mimetic effect in the lipogenesis assay and in the glycerol release lipolysis assay. On the other hand, in the lipolysis assay based on the release of free fatty acids, all of the complexes do have an effect, suggesting that here the conditions allowed for the (at least partial) incorporation of the vanadium complexes. Particularly efficient in the FFA release assay is the mixed ligand complex [V^V(pic-trpH)tpa]$^{2+}$ (**4**), and complex **5** ([V^VO(pic-trpMe)$_2$]$^{2+}$) with a less rigid overall ligand system.

Experimental

General and instrumentation

All synthetic procedures for the oxidovanadium complexes were performed under an atmosphere of dry nitrogen using standard Schlenk and vacuum-line techniques. The solvents were dried by distillation over appropriate drying agents and kept over molecular sieves under nitrogen. All chemicals were used as received. NMR spectra were recorded on a Varian Inova 500 MHz, Bruker AVANCE 400 MHz or Varian Gemini-200 MHz spectrometer, using the solvent resonance or trimethylsilane, TMS, as an internal standard for the ^{1}H NMR, and $VOCl_3$ as an external standard for ^{51}V NMR. EPR spectra were run in the X-band mode at 9.4–9.5 GHz on a Bruker ESP 300E spectrometer. Simulations were carried out with the program system WinEPR SimFonia.[35] IR spectra were recorded in KBr pellets on a Nicolet Avatar 360 and a Perkin Elmer 1720 FT-IR instrument. Electrospray (ES) mass spectra were obtained on acetonitrile solutions using a Waters micromass ZQ 4000 mass spectrometer working in the positive mode, with a source temperature of 80 °C and desolvation temperature of 120 °C. Fast atom bombardment (FAB; with xenon) mass spectra were recorded on a VG 70–250 S Analytical instrument in a *m*-nitrobenzyl alcohol (*m*-NBA) matrix. Cyclic voltammograms were obtained with an eDAQ model 160 potentiostat equipped with a model 401 e-corder, using a Pt button working electrode, a Pt wire counter electrode, and a Ag/AgCl reference electrode. Tetrabutylammonium perchlorate was used as a supporting electrolyte. CH_2Cl_2, dried over a

Table 5 Crystal data and structure refinement for **1** and **2**·MeOH

	[VO(bp-O)HSO$_4$] **1**	[VO(bp-OH)Cl$_2$]·MeOH **2**·MeOH
Empirical formula	$C_{19}H_{19}N_3O_6SV$	$C_{20}H_{23}Cl_2N_3O_3V$
Formula weight/g mol^{-1}	468.37	475.25
T/K	120(2)	120(2)
λ/Å	0.71073 Å	0.71073 Å
Crystal system	Monoclinic	Orthorhombic
Space group	$P2_1/c$	$P2_12_12_1$
Unit cell dimensions		
a/Å	17.7424(4)	8.2798(4)
b/Å	7.8207(3)	14.8063(6)
c/Å	14.2763(6)	17.2853(7)
β/°	103.265(3)	
V/Å^3	1928.10(12)	2119.06(16)
Z	4	4
D_{calcd}/Mg m^{-3}	1.614	1.490
Θ range/°	2.86 to 28.72	2.73 to 27.45°.
F(000)	964	980
Reflexions, independent refl. (R_{int})	20463, 4975 [R(int) = 0.0524]	18593, 4826 [R(int) = 0.0508]
Restraints, parameters	0, 272	0, 266
$R1$ ($wR2$) [$I>2\sigma(I)$]	0.0392 (0.0832)	0.0355 (0.0721)
$R1$ ($wR2$) for all data	0.0777 (0.0953)	0.0550 (0.0788)
Largest diff. peak and hole/e Å^{-3}	0.401 and –0.442	0.276 and –0.231

molecular sieve, was deoxygenated by passage of a N_2 stream through the solution. The ferrocene redox couple (0.400 V *vs.* NHE) was employed as an internal standard.

The crystals of **1** and **2** were immersed in cryo-oil, mounted in a Nylon loop, and measured at 120 K. The X-ray diffraction data was collected by means of a Nonius KappaCCD diffractometer using Mo Kα radiation (λ = 0.71073 Å). The Denzo-Scalepack[36] program package was used for cell refinements and data reductions. The structure was solved by direct methods using the SHELXS-97[37] program with the WinGX[38] graphical user interface. A semi-empirical absorption correction (SADABS)[39] was applied to the data. Structural refinements were carried out using SHELXL-97.[40] The OH hydrogen in **2** was located from the difference Fourier map but constrained to ride on its parent atom, with U_{iso} = 1.5 U_{eq} (parent atom). Other hydrogens were positioned geometrically and constrained to ride on their parent atoms, with C–H = 0.95–0.99 Å and U_{iso} = 1.2–1.5 U_{eq} (parent atom). Table 5 summarises the crystal and structure refinement data.

EPR measurements and computational details

EPR spectra were recorded with a Bruker X-band (9.4–9.5 GHz) ESP 300E spectrometer at room temp. (isotropic spectra) or at liquid nitrogen temp. (anisotropic spectra). The parameters reported in Table 2 were obtained by simulating the EPR spectrum of each species present in solution, considering that the percentage amount of the predominant species is 90% and that of the minor one is 10%. In all the simulations, second-order effects were taken into account, the x,y,z line widths were set to 10 Gauss and the ratio Lorentzian/Gaussian, affecting the line shape, to 1.

All of the calculations presented in this paper were performed using the Gaussian 03 program (revision C.02)[41] and DFT methods.[25] The geometry of the complexes was optimised (keyword = Opt) without symmetry constraints using the hybrid exchange–correlation B3LYP functional,[42,43] and the 6-311g basis set. Frequency calculations (keyword = Freq) were subsequently performed in order to verify that all the structures were local minima on the potential *energy* surface with real frequencies.

The ^{51}V hyperfine coupling constants (A_{iso}, A_x, A_y and A_z) were calculated from the optimised structures with the half-and-half functional BHandHLYP and 6-311g(d,p) basis sets. BHandHLYP was used as incorporated in Gaussian 03, and includes a mixture of the exact Hartree–Fock exchange energy and of that obtained from DFT methods to calculate the exchange–correlation energy:[43] $E_{XC} = 0.5*E_X^{HF} + 0.5*E_X^{LSDA} + 0.5*E_X^{B} + E_C^{LYP}$, where E_X^{HF}, E_X^{LSDA}, E_X^{B} and E_C^{LYP} are the energies due to the Hartree–Fock exchange, to the Local Spin Density Approximation (LSDA) exchange functional,[44] to the gradient-corrected Becke 88 (B) exchange functional,[45] and to the gradient-corrected Lee–Yang–Parr (LYP) correlation functional,[43] respectively. The performances of the BHandHLYP functional were recently tested on 22 representative V^{IV}O complexes with different charges, geometries and coordination modes, and a mean deviation of A_z from the experimental value of 2.7% was found.[27]

Syntheses

Ligand syntheses. The following pro-ligands/ligands were synthesised according to published procedures: tpa,[20] picMe-trpMe,[12] picH-OEt.[30]

The ligand bp-OH was prepared by a modification of a previously described route:[23a,46] *o*-cresol was condensed with 1.5 equivalents of acetic anhydride. The product was purified by vacuum distillation and refluxed with a 1.4-fold excess of *N*-bromosuccinimide plus a trace of benzoyl peroxide in CH_2Cl_2 for 30 h. The 2-bromomethylphenyl acetate thus formed was stirred with an equivalent amount of dipicolylamine, plus a 2.5-fold excess of triethylamine in ethyl acetate at room temperature for six days. De-acylation, carried out with NaOH, followed by purification on a silica gel column, using ethyl acetate/triethylamine 9/1 as eluent, gave a yellow solid of bp-OH, as confirmed by ^{1}H-NMR spectroscopy, in 33% yield.

Complexes

The following complexes were prepared according to literature procedures: [VO(tpa)SO$_4$] (**3**),[20] [VO(pic-trpMe)$_2$] (**5**).[12]

[V^{IV}O(bp-O)HSO$_4$] (1). This complex was synthesised by a method similar to the one described for the corresponding tpa (*tris*(2-pyridylethyl)amine) complex.[20] A 10 mL solution of bp-OH (0.21 g, 0.68 mmol) in methanol was added to a 10 mL methanol solution of VO(SO$_4$)·5H$_2$O (0.17 g, 0.69 mmol). After stirring over night at room temp., a brownish solution was obtained. The solvent volume was reduced to *ca.* 3 mL, and the resulting concentrated solution was layered with diethyl ether. Dark purple parallel sheet-like crystals grew at the interface and were filtered off. Yield 0.283 g (84%). IR (KBr, cm^{-1}): ν(V=O) 971, ν(HSO$_4$) 1158. MS (ES+): m/z 371 ([VO(bp-O)]), 402 weak ([VO(bp-O)]·MeOH). Elemental analysis (%) calcd for $C_{19}H_{19}N_3O_6SV$; M = 468.38 g mol^{-1}: C 48.72, H 4.09, N 8.97, S 6.85. Found: C 47.95, H 4.51, N 8.68, S 7.01. UV-vis (nm (ε/M^{-1} cm^{-1})) in H$_2$O: 765 (42), 533 (57). For EPR data see Table 2.

[$V^{IV}O$(bp-OH)Cl_2]·CH_3OH (2·CH_3OH). $VOSO_4 \cdot 5H_2O$ (0.14 g, 0.60 mmol) and $BaCl_2 \cdot 2H_2O$ (0.15 g, 0.60 mmol) were stirred together in 10 mL of methanol for a *ca.* 3 h. Formed solid $BaSO_4$ was separated by centrifugation, and the solution was added to a 10 mL methanol solution of bp-OH (0.18 g, 0.60 mmol). The reaction mixture was stirred over night at room temp., resulting in a brownish solution. The solvent volume was reduced, and the resulting concentrated solution was layered with diethyl ether. Within three days, green thin spicular crystals formed. Yield 0.254 g (88%). IR (KBr, cm^{-1}): ν(V=O) 975. MS (ES+): *m*/*z* 407 ([VO(bp-O)Cl]), 306 (bp-OH). Elemental analysis (%) calcd for $C_{20}H_{23}Cl_2N_3O_3V$; M = 475.27 g mol^{-1}: C 50.54, H 4.88, N 8.84. Found: C 50.31, H 5.29, N 8.62. UV-vis (nm (ε/M^{-1} cm^{-1})) in H_2O: 764 (45), 525 (61). For EPR data see Table 2.

[VO(pic-trpH)tpa]Cl_2 (4Cl_2). The pro-ligand picMe-trpMe (0.98 g, 2.56 mmol) was dissolved in 10 mL of methanol, treated with KOH (0.45 g, 8.00 mmol), and stirred for 4 h at 60 °C. The reaction mixture was cooled back to room temp., and the acidity adjusted to pH = 3 by addition of 1 M HCl. Solvents were removed *in vacuo*, the deprotected ligand picH-trpH was extracted from the residue with $CHCl_3$, and the chloroform was removed by evaporation. The co-ligand tpa (81 mg, 0.28 mmol) was treated with hydrochloric acid and the resulting hydrochloride tpa·HCl suspended in 5 mL of THF. To this suspension, 2 mL of a methanol solution containing [VO(O*i*Pr)$_3$] (68 mg, 0.28 mmol) was added dropwise over a period of 1 h. The reaction mixture was stirred for 1 day at room temp. and then treated with picH-trpH (100 mg, 0.28 mmol) dissolved in 3 mL of methanol. The precipitate obtained after brief stirring was filtered off and recrystallised from methanol/toluene 1/1. Yield 164 mg (0.21 mmol, 75%). IR (KBr, cm^{-1}): ν(C=O) 1713; $\nu_{as}(CO_2^-)$, 1608, 1573; $\nu_s(CO_2^-)$ 1380, 1351; ν(V=O) 978. ^{51}V NMR ($CDCl_3$/MeOH 3/1) δ: –485. Elemental analysis (%) calcd for $C_{36}H_{32}Cl_2N_7O_6V$; M = 780.54 g mol^{-1}: C 58.49, H 4.53, N 11.48. Found: C 58.51, H 4.19, N 11.30.

[VO(pic-OEt)tpa]Cl_2 (6Cl_2). 5-Carboethoxypyridine-2-carboxylic acid, picH-OEt (25 mg, 0.13 mmol), was converted to its corresponding hydrochloride salt picH-OEt·HCl, dissolved in 3 mL of $CHCl_3$ and treated with [VO(O*i*Pr)$_3$] (29 mg, 0.13 mmol). To this solution was added, within one h, 5 mL of a chloroform solution of tpa (37 mg, 0.13 mmol). The reaction mixture was stirred for *ca*. 5 min, after which the solution was reduced to about one third of its original volume and treated with hexane. The precipitate thus obtained was filtered off and recrystallised from chloroform/acetone 1/1. Yield: 68 mg (0.11 mmol, 85%). IR (KBr, cm^{-1}): ν(C=O) 1722; $\nu_{as}(CO_2^-)$, ν(C=C), ν(C=N) 1606, 1570, 1483, 1442; $\nu_s(CO_2^-)$ 1353; ν(V=O) 940. MS (*m*-NBA, FAB): *m*/*z* (%) 745 (1) ([VO(pic-OEt)$_2$tpa]), 551 (65) [VO(pic-OEt)tpa]. ^{51}V NMR ($CDCl_3$, δ): –489. Elemental analysis (%) calcd for $C_{27}H_{27}Cl_2N_5O_5V$; M = 623.39 g mol^{-1}: C 52.11, H 4.21, N 11.25. Found: C 52.53, H 4.25, N 11.35.

Speciation and evaluation of insulin mimetic properties

Speciation studies

The exact concentration of the ligand stock solution was determined by the Gran method.[47] The VO^{2+} stock solution (c = 0.04152 M, HCl content 0.0906 M) was prepared as described,[48] and standardised for the metal ion concentration by permanganate titration.

pH-potentiometric measurements for determining the stability constants of the VO^{2+} complexes and of the ligands were carried out at an ionic strength of 0.2 M (KCl) and at 25.0 °C in DMSO:water 20:80 (w/w); pK_w = 14.206 ± 0.37%. The titrations were performed with 0.2 M carbonate-free KOH. Both the base and the HCl used were Reanal products, and their concentrations were determined by pH-metric titrations. An Orion 710A pH meter equipped with a Metrohm combined electrode (type 6.0234.100) and a Metrohm 665 Dosimat burette were used for the pH-metric measurements, performed in the pH range of 2–12. The electrode system was calibrated according to Irving *et al.*[49] The samples were completely deoxygenated by bubbling purified argon through the solutions for *ca.* 10 min prior to the measurements, and argon was also passed across the solutions during the titrations.

Dissociation constants of the compounds were determined with the computer program SUPERQUAD;[50] and PSEQUAD[51] was utilised to establish the stoichiometry of the complexes and to calculate the stability constants logβ[$(VO)_pL_qH_r$].

Lipogenesis assay

Adipocytes were isolated from epididymal fat pads of 36–38 days old male Sprague Dawley rats and prepared as described previously.[52,53] The lipogenesis assay follows the one previously described by Moody *et al.*:[54] 1 mL aliquots of 2% (v/v) adipocytes in Krebs-Ringer-Hepes (KRH) buffer with low glucose (0.55 mM) and 3.5% bovine serum albumin (BSA) were added to vials containing 0.4 μCi D-[6–^{3}H]-glucose, and incubated with either insulin (1.7 nM), Na_3VO_4 (5 mM), $VOSO_4$ (in the concentration range 10 μM to 5 mM), [$V^{IV}O$(tpa)SO_4] (**3**), [$V^{IV}O$(bp-O)HSO_4] (**1**) or [$V^{IV}O$(bp-OH)Cl_2]·MeOH (**2**·MeOH) (1 μM to 5 mM) for 0.5–3 h at 37 °C. Reactions were stopped by addition of a toluene-based scintillation liquid containing 0.3 g/L 1,4-bis[5-phenyl-2-oxazolyl]benzene, 2,2′-*p*-phenylene-bis[5-phenyloxazole] (POPOP) and 5 g/L 2,5-diphenyl oxazole (PPO). Incorporation of D-[6–^{3}H]-glucose into cellular lipids was measured by scintillation counting.

Lipolysis assays

Glycerol release. Glycerol release was measured as previously described:[54] 400 μL aliquots of 5% (v/v) adipocytes in KRH buffer were incubated with isoprenaline (100 nM) and either insulin (1.7 nM), $VOSO_4$ (500 μM), [$V^{IV}O$(tpa)SO_4] (**3**), [$V^{IV}O$(bp-O)HSO_4] (**1**) or [$V^{IV}O$(bp-OH)Cl_2]·MeOH (**2**·MeOH) (250 μM) for 30 min at 37 °C. The reactions were stopped by putting the tubes on ice for 20 min. 1 mL of hydrazine buffer (50 mM glycine pH 9.8, 0.05% hydrazine hydrate, 1 mM $MgCl_2$, supplemented with 0.75 mg/mL adenosine triphosphate (ATP), 0.375 mg/mL nicotinamide adenine dinucleotide (NADP), 25 μg/mL glycerol-3-phosphate dehydrogenase and 0.5 μg/mL glycerolkinase) was added to the 200 ml of the combined media. After incubation for 40 min at room temp., the optical density was measured at 340 nm. The animal experiments in the lipogenesis and the glycerol release

assay were approved by the Lund University Ethical Committee (permission number: 158–06).

Release of free fatty acids (FFA).[31,55] Male Wistar rats were sacrificed under anaesthesia with ether. The adipose tissues were removed, chopped and digested with collagenase for 60 min at 37 °C in KR bicarbonate buffer (120 mM NaCl, 1.27 mM $CaCl_2$, 1.2 mM $MgSO_4$, 4.75 mM KCl, 1.2 mM KH_2PO_4, 24 mM $NaHCO_3$: pH 7.4), containing 2% BSA. The adipocytes were then separated from undigested tissues by filtration through nylon mesh and washed three times. The vanadium complexes or ligands were dissolved in saline solutions at various concentrations (final conc. 0.1, 0.5, and 1 mM); 30 μL of each solution and 15 μL of glucose (final conc. 5 mM) were added to 240 μL of the isolated adipocytes, and the resulting suspensions were incubated at 37 °C for 30 min. Finally, 15 μL of epinephrine solution (final conc. 10 μM) was added to the reaction mixtures, and the resulting solutions were incubated at 37 °C for 180 min. The reactions were stopped by soaking in ice water, and the mixtures were centrifuged at 3000 rpm for 10 min. FFA levels in the outer solution of the cells were determined using an FFA kit (NEFA C-test WAKO, Wako Pure Chemicals). The animal experiments in the FFA study were approved by the Experimental Animal Research of Kyoto Pharmaceutical University (KPU), and were performed according to the Guidelines for Animal Experimentation of KPU.

Acknowledgements

This research has been supported by grants from the Research School for Pharmaceutical Sciences (http://www.flak.lu.se, to EN), the Swedish Foundation for International Cooperation in Research and Higher Education (STINT, to JN and EN) and the Deutsche Akademische Austauschdienst (DAAD, to HE and DR). We thank Eva Ohlson for technical assistance.

References

1 D. Rehder, *Bioinorganic Vanadium Chemistry*, Wiley & Sons, Chichester, 2008.
2 M. D. Cohen, *Toxicol. Ecotoxicol. News*, 1996, **3**, 132.
3 (*a*) L. C. Cantley Jr., L. Josephson, R. Warner, M. Yanagisawa, C. Lechene and G. Guidotti, *J. Biol. Chem.*, 1977, **252**, 7421; (*b*) M. J. Gresser and A. S. Tracey, in: *Vanadium in Biological Systems*, ed. N. D. Chasteen, Kluwer Academic Publishers, Dordrecht, 1990, ch. IV.; (*c*) G. L. Mendz, *Arch. Biochem. Biophys.*, 1991, **291**, 201.
4 (*a*) M. A. Andersson and S. G. Allenmark, *Tetrahedron*, 1998, **54**, 15293; (*b*) H. B. ten Brink, H. E. Schoemaker and R. Wever, *Eur. J. Biochem.*, 2001, **268**, 132.
5 (*a*) R. L. Robson, R. R. Eady, T. H. Richardson, R. W. Miller, M. Hawkins and J. R. Postgate, *Nature*, 1986, **322**, 388; (*b*) R. R. Eady, *Coord. Chem. Rev.*, 2003, **237**, 23.
6 B. Lyonnet, X. Mertz and E. Martin, *Presse Med.*, 1899, **1**, 191.
7 (*a*) E. L. Tolman, E. Barris, M. Burns, A. Pansini and R. Partridge, *Life Sci.*, 1979, **25**, 1159; (*b*) Y. Shechter and S. J. Karlish, *Nature*, 1980, **284**, 556.
8 (*a*) C. E. Heyliger, A. G. Tahili and J. H. McNiell, *Science*, 1985, **227**, 1474; (*b*) O. Blondel, D. Bailbe and B. Portha, *Diabetologia*, 1989, **32**, 185.
9 (*a*) B. I. Posner, R. Faure, J. W. Burgess, A. P. Bevan, D. Lachance, G. Zhang-Sun, I. G. Fantus, J. B. Ng, D. A. Hall, B. Soo Lum and A. Shaver, *JBIC, J. Biol. Inorg. Chem.*, 1994, **269**, 4596; (*b*) H. Ou, L. Yan, D. Mustafi, M. W. Makinen and M. J. Brady, *JBIC, J. Biol. Inorg. Chem.*, 2005, **10**, 874.
10 I. Goldwasser, D. Gefel, E. Gershonov, M. Fridkin and Y. Schechter, *J. Inorg. Biochem.*, 2000, **80**, 21.
11 B. D. Liboiron, K. H. Thompson, G. R. Hnson, E. Lam, N. Aebischer and C. Orvig, *J. Am. Chem. Soc.*, 2005, **127**, 4194.
12 H. Esbak, E. A. Enyedy, T. Kiss, Y. Yoshikawa, H. Sakurai, E. Garribba and D. Rehder, *J. Inorg. Biochem.*, 2009, **103**, 590.
13 T. C. Delgado, A. I. Tomaz, I. Corriera, J. Costa Pessoa, J. G. Jones, C. F. G. C. Geraldes and M. M. C. A. Castro, *J. Inorg. Biochem.*, 2005, **99**, 2328.
14 Marzban and J. H. McNeill, *J. Trace Elem. Exp. Med.*, 2003, **16**, 253.
15 (*a*) A. P. Bevan, P. G. Drake, J.-F. Yale, A. Shaver and B. I. Posner, *Mol. Cell. Biochem.*, 1995, **153**, 49; (*b*) H. Sakurai, A. Katoh and Y. Yoshikawa, *Bull. Chem. Soc. Jpn.*, 2006, **79**, 1645.
16 H. Sakurai and A. Tsuji, in: *Vanadium in the Environment*, ed. J. O. Nriagu, John Wiley & Sons, New York, 1998, part 2, p. 297.
17 Y. Zhang, X.-D. Yang, K. Wang and D. C. Crans, *J. Inorg. Biochem.*, 2006, **100**, 80.
18 K. H. Thompson, B. D. Liboiron, Y. Sun, K. D. D. Bellman, I. A. Setyawati, B. O. Patrick, V. Karunaratne, G. Rawji, J. Wheeler, K. Sutton, S. Bhanot, C. Cassidy, J. H. McNeill, V. G. Yuen and C. Orvig, *JBIC, J. Biol. Inorg. Chem.*, 2003, **8**, 66.
19 (*a*) Akesis Pharmaceuticals (San Diego), http://www.akesis.com; (*b*) K. H. Thompson, J. Lichter, C. LeBel, M. C. Scaife, J. H. McNeill and C. Orvig, *J. Inorg. Biochem.*, 2009, **103**, 554.
20 Y. Tajika, K. Tsuge and Y. Sasaki, *Dalton Trans.*, 2005, 1438.
21 M. R. Caira, J. M. Haigh and L. R. Nassimbeni, *J. Inorg. Nucl. Chem.*, 1972, **34**, 3171.
22 D. Rehder, T. Polenova and M. Bühl, *Annu. Rep. NMR Spectrosc.*, 2007, **62**, 114.
23 (*a*) A. Thapper, A. Behrens, J. Fryxelius, M. H. Johansson, F. Prestopino, M. Czaun, D. Rehder and E. Nordlander, *Dalton Trans.*, 2005, 3566; (*b*) M. Velusamy, R. Mayilmurugan and M. Palaniandavar, *Inorg. Chem.*, 2004, **43**, 6284.
24 (*a*) N. D. Chasteen, in: *Biological Magnetic Resonance*, ed. L. J. Berliner and J. Reuben, Plenum Press, New York, USA, vol. 3, 1981, p. 53.; (*b*) T. S. Smith II, R. LoBrutto and V. L. Pecoraro, *Coord. Chem. Rev.*, 2002, **228**, 1; (*c*) E. Garribba, E. Lodyga-Chruscinska, G. Micera, A. Panzanelli and D. Sanna, *Eur. J. Inorg. Chem.*, 2005, 1369.
25 (*a*) R. G. Parr and W. Yang, *Density-Functional Theory of Atoms and Molecules*, Oxford University Press, Oxford, United Kingdom, 1989; (*b*) *Calculation of NMR and EPR Parameters. Theory and Applications*, ed. M. Kaupp, M. Bühl and V. G. Malkin, Wiley-VCH, Weinheim, Germany, 2004.
26 (*a*) F. Neese, *J. Chem. Phys.*, 2003, **118**, 3939; (*b*) M. L. Munzarová and M. Kaupp, *J. Phys. Chem. B*, 2001, **105**, 12644, and references therein; (*c*) A. C. Saladino and S. C. Larsen, *J. Phys. Chem. A*, 2003, **107**, 1872.
27 G. Micera and E. Garribba, *Dalton Trans.*, 2009, 1914.
28 H. Kumagai, M. Endo, M. Kondo, S. Kawata and S. Kitagawa, *Coord. Chem. Rev.*, 2003, **237**, 197.
29 S. A. Ross, E. A. Gulve and M. Wang, *Chem. Rev.*, 2004, **104**, 1255.
30 F. Moller and M. W. Roomi, *Anal. Biochem.*, 1974, **59**, 248.
31 M. Nakai, H. Watanabe, C. Fujiwara, H. Kagegawa, T. Satoh, J. Takada, R. Matsushita and H. Sakurai, *Biol. Pharm. Bull.*, 1995, **18**, 719.
32 K. H. Thompson, J. Leichter and J. H. McNeill, *Biochem. Biophys. Res. Commun.*, 1993, **197**, 1549.
33 (*a*) E. J. Baran, *J. Carbohydr. Chem.*, 2001, **20**, 769; (*b*) B. Baruah, S. Das and A. Chakravorty, *Coord. Chem. Rev.*, 2003, **237**, 135; (*c*) D. A. Barrio, E. R. Cattaneo, M. C. Apezteguia and S. B. Etcheverry, *Can. J. Physiol. Pharmacol.*, 2006, **84**, 765.
34 K. Kawabe, T. Suekuni, T. Inada, K. Yamato, M. Tadokoro, Y. Kojima, Y. Fujisawa and H. Sakurai, *Chem. Lett.*, 1998, **21**, 1155.
35 *WINEPR SimFonia*, version 1.25, Bruker Analytische Messtechnik GmbH, Karlsruhe, 1996.
36 Z. Otwinowski and W. Minor, *Processing of X-ray Diffraction Data Collected in Oscillation Mode*, Academic Press, New York, 1997, p. 307.
37 G. M. Sheldrick, *SHELXS-97, Program for Crystal Structure Determination*, University of Göttingen, Göttingen, Germany, 1997.
38 L. J. Farrugia, *J. Appl. Crystallogr.*, 1999, **32**, 837.
39 G. M. Sheldrick, *SADABS – Bruker Nonius scaling and absorption correction*, v 2.10, Bruker AXS, Inc., Madison, Wisconsin, USA, 2003.
40 G. M. Sheldrick, *SHELXL-97, Program for Crystal Structure Refinement*, University of Göttingen, Göttingen, Germany, 1997.
41 M. J. Frisch, G. W. Trucks, H. B. Schlegel, G. E. Scuseria, M. A. Robb, J. R. Cheeseman, J. A. Montgomery, Jr., T. Vreven, K. N. Kudin, J. C.

Burant, J. M. Millam, S. S. Iyengar, J. Tomasi, V. Barone, B. Mennucci, M. Cossi, G. Scalmani, N. Rega, G. A. Petersson, H. Nakatsuji, M. Hada, M. Ehara, K. Toyota, R. Fukuda, J. Hasegawa, M. Ishida, T. Nakajima, Y. Honda, O. Kitao, H. Nakai, M. Klene, X. Li, J. E. Knox, H. P. Hratchian, J. B. Cross, V. Bakken, C. Adamo, J. Jaramillo, R. Gomperts, R. E. Stratmann, O. Yazyev, A. J. Austin, R. Cammi, C. Pomelli, J. Ochterski, P. Y. Ayala, K. Morokuma, G. A. Voth, P. Salvador, J. J. Dannenberg, V. G. Zakrzewski, S. Dapprich, A. D. Daniels, M. C. Strain, O. Farkas, D. K. Malick, A. D. Rabuck, K. Raghavachari, J. B. Foresman, J. V. Ortiz, Q. Cui, A. G. Baboul, S. Clifford, J. Cioslowski, B. B. Stefanov, G. Liu, A. Liashenko, P. Piskorz, I. Komaromi, R. L. Martin, D. J. Fox, T. Keith, M. A. Al-Laham, C. Y. Peng, A. Nanayakkara, M. Challacombe, P. M. W. Gill, B. G. Johnson, W. Chen, M. W. Wong, C. Gonzalez and J. A. Pople, *GAUSSIAN 03 (Revision C.02)*, Gaussian, Inc., Wallingford, CT, 2004.
42 A. D. Becke, *J. Chem. Phys.*, 1993, **98**, 5648.
43 C. Lee, W. Yang and R. G. Parr, *Phys. Rev. B*, 1988, **37**, 785.
44 A. D. Becke, *Phys. Rev. A*, 1988, **38**, 3098.
45 S. H. Vosko, L. Wilk and M. Nusair, *Can. J. Phys.*, 1980, **58**, 1200.
46 S. Wang, L. Wang, X. Wang and Q. Lou, *Inorg. Chim. Acta*, 1997, **254**, 71.
47 G. Gran, *Acta Chem. Scand.*, 1950, **4**, 559.
48 I. Nagypál and I. Fábián, *Inorg. Chim. Acta*, 1982, **61**, 109.
49 H. M. Irving, M. G. Miles and L. D. Pettit, *Anal. Chim. Acta*, 1967, **38**, 475.
50 A. Sabatini, A. Vacca and P. Gans, *Talanta*, 1974, **21**, 53.
51 L. Zékány and I. Nagypál, *Computational Methods for the Determination of Stability Constants*, ed. D. L. Leggett, Plenum Press, New York, 1985, p. 291.
52 R. C. Honnor, G. S. Dhillon and C. J. Londos, *Biochem. Soc. Trans.*, 1990, **18**, 1123.
53 V. Dole and H. Neinerts, *J. Biol. Chem.*, 1960, **235**, 2595.
54 A. J. Moody, M. A. Stan, M. Stan and J. Glieman, *Horm. Metab. Res.*, 1974, **6**, 12.
55 J. Gätjens, B. Meier, T. Kiss, E. M. Nagy, P. Buglyó, H. Sakurai, K. Kawabe and D. Rehder, *Chem.–Eur. J.*, 2003, **9**, 4924.